


# Super-ballistic diffusion in a quasi-periodic non-Hermitian driven system with nonlinear interaction

Jian-Zheng Li(李建政), Guan-Ling Li(李观玲), and Wen-Lei Zhao(赵文垒)
**Citation:**Chin. Phys. B, 2023, 32 (**9**): 096601. DOI: 10.1088/1674-1056/acd2af
Journal homepage: http://cpb.iphy.ac.cn; http://iopscience.iop.org/cpb

**What follows is a list of articles you may be interested in**

---

## Molecular dynamics simulation of thermal conductivity of silicone rubber

Wenxue Xu(徐文雪), Yanyan Wu(吴雁艳), Yuan Zhu(祝渊), Xin-Gang Liang(梁新刚)
Chin. Phys. B, 2020, 29 (**4**): 046601. DOI: 10.1088/1674-1056/ab7743

## Radial transport dynamics studies of SMBI with a newly developed TPSMBI code

Ya-Hui Wang(王亚辉), Wen-Feng Guo(郭文峰), Zhan-Hui Wang(王占辉), Qi-Long Ren(任启龙), Ai-Ping Sun(孙爱萍), Min Xu(许敏), Ai-Ke Wang(王爱科), Nong Xiang(项农)
Chin. Phys. B, 2016, 25 (**10**): 106601. DOI: 10.1088/1674-1056/25/10/106601

## Surface-charge-governed electrolyte transport in carbon nanotubes

Xue Jian-Ming (薛建明), Guo Peng (郭鹏), Sheng Qian (盛倩)
Chin. Phys. B, 2015, 24 (**8**): 086601. DOI: 10.1088/1674-1056/24/8/086601

## Molecular dynamics study of thermal stress and heat propagation in tungsten under thermal shock

Fu Bao-Qin (付宝勤), Lai Wen-Sheng (赖文生), Yuan Yue (袁悦), Xu Hai-Yan (徐海燕), Li Chun (李纯), Jia Yu-Zhen (贾玉振), Liu Wei (刘伟)
Chin. Phys. B, 2013, 22 (**12**): 126601. DOI: 10.1088/1674-1056/22/12/126601

---

# Super-ballistic diffusion in a quasi-periodic non-Hermitian driven system with nonlinear interaction

Jian-Zheng Li(李建政), Guan-Ling Li(李观玲), and Wen-Lei Zhao(赵文垒)[†]

*School of Science, Jiangxi University of Science and Technology, Ganzhou* 341000, *China*

(Received 10 November 2022; revised manuscript received 16 April 2023; accepted manuscript online 5 May 2023)

We investigate the effects of nonlinear interactions on quantum diffusion in a quasi-periodic quantum kicked rotor system, featuring a non-Hermitian kicking potential. Remarkably, when the non-Hermitian driving strength is sufficiently strong, the energy diffusion follows a power law of time, characterized by an exponent that decreases monotonically with increasing the strength of nonlinear interactions. This demonstrates the emergence of super-ballistic diffusion (SBD). We find a distinct prethermalization stage in the time domain preceding the onset of SBD. The unique quantum diffusion phenomena observed in this chaotic system can be attributed to the decoherence effects generated by the interplay between nonlinear interactions and the non-Hermitian kicking potential.

**Keywords:** super-ballistic diffusion, Bose–Einstein condensate, nonlinear interaction, non-Hermiticity

**PACS:** 66.10.cd, 67.85.Hj, 05.45.–a **DOI:** 10.1088/1674-1056/acd2af

## 1. Introduction

Quantum diffusion of Floquet-driven systems[1–6] has garnered significant attention across various fields of physics, including quantum chaos and condensed matter physics.[7–15] The quantum kicked rotor (QKR), a paradigmatic model of quantum chaos, exhibits a well-known phenomenon of dynamical localization (DL),[16,17] which is analogous to Anderson localization of electrons in disordered lattices.[18,19] The quasi-periodic quantum kicked rotor (QPQKR) with $N$ incommensurable frequencies, a variant of the QKR model induced by modulating the kicking potential, can emulate the $N$-dimensional Anderson model in coordinate representation,[16,20,21] offering an ideal platform for verifying the scaling law of Anderson transitions. Theoretical investigations on quantum diffusion of the QPQKR have been observed in state-of-the-art experiments involving Bose–Einstein condensates (BEC) of ultra-cold atoms.[22–28] Previous investigations have shown that the nonlinear interaction of BEC atoms, a mean-field approximation of many-body interaction, induces sub-diffusion in the QPQKR model governed by the Gross–Pitaevskii (GP) equation.[29–35]

It is widely recognized that an open system interacting with its environment can be described by a non-Hermitian Hamiltonian.[36–40] The non-Hermitian extension to Floquet-driven systems has stimulated numerous studies on quantum diffusion behaviors.[41–44] For instance, when a general non-Hermitian driving potential is introduced to coupled QKRs, the phenomenon of DL is effectively protected due to novel quantum coherence.[45] Interestingly, when a $\mathcal{PT}$-symmetric non-Hermitian driving potential is applied to a QKR system with nonlinear interaction, super-exponential diffusion emerges as a result of the non-Hermitian modulation of the nonlinear interaction.[46] In this context, the diffusion behaviors arising from the interplay between nonlinearity and non-Hermiticity in the QPQKR model deserve urgent investigation.

In this work, we investigate the quantum diffusion of BEC by utilizing a nonlinear and non-Hermitian extension of the QPQKR model. When the strength of the non-Hermitian driving potential is weak, the system displays two classes of energy diffusion, namely the DL and subdiffusion (SD) corresponding to weak and strong nonlinear interactions, respectively. As the non-Hermitian parameter is sufficiently large, we can find a transition from SBD to AD and then to CD with the increase of nonlinearity. We numerically ascertain the diffusion exponent and the diffusion coefficient of mean energy across a broad range of system parameters, which can is useful for the Floquet engineering of energy diffusion. Notably, we identify a prethermalization stage preceding the emergence of SBD. Through the analysis of the norm ($\mathcal{N}$), we further unveil that the interplay between the non-Hermitian driving potential and the nonlinear interaction underlies the SBD phenomenon.

The paper is structured as follows: In Section 2, we present the QPQKR model of BEC, incorporating nonlinearity and non-Hermiticity. In Section 3, we explore the diffusion behavior within this system, focusing particularly on the SBD behavior, and discuss its underlying mechanism. A summary is presented in Section 4.

## 2. Theoretical model

We consider a system of ultra-cold atoms confined in a ring trap with radius of $R$ and subjected to quasi-periodic

[†]Corresponding author. E-mail: wlzhao@jxust.edu.cn

© 2023 Chinese Physical Society and IOP Publishing Ltd 

$\delta$ kicks of optical standing wave with complex dielectric constants.[47–49] The Hamiltonian of the QPQKR model reads

$$H = \frac{p^2}{2} + g|\psi(p)|^2 + V_{\rm K}(\theta)\sum_{n=0}^{\infty}\delta(t-n), \tag{1}$$

with the quasi-periodic kicking potential

$$V_{\rm K} = (K + {\rm i}\lambda)[1+\varepsilon\cos(\omega t)]\cos\theta, \tag{2}$$

where $\theta$ is the angle coordinate. We take $\hat{p} = -{\rm i}\hbar_{\rm eff}\partial/\partial\theta$ as the corresponding angular momentum operator, with $\hbar_{\rm eff}$ being the effective Planck constant and satisfying the commutation relation $[\theta, \hat{p}] = {\rm i}\hbar_{\rm eff}$. The nonlinear interaction strength is denoted by $g$, while $K$ and $\lambda$ control the strength of the real and imaginary parts of the kicking, respectively. Additionally, $\varepsilon$ is the quasi-periodic modulation strength for the kicking potential. When the modulation frequency is incommensurable with the kicking frequency, ensured by $\omega = 2\pi r/s$ with $r$ and $s$ being coprime numbers, the QPQKR model can mimic the 2D Anderson model.[20,21] Here, $\omega = 2\pi e$. All variables are scaled to dimensionless units. It is worth noting that the QPQKR model in the Hermitian case (i.e., $\lambda = 0$) has been utilized to demonstrate the nonlinearity induced sub-diffusion of energy.[20,21]

One can expand an arbitrary quantum state $|\psi\rangle$ using the eigenstates of angular momentum operators as $|\psi\rangle = \sum_m \psi_m|\phi_m\rangle$, with the eigenequation $p|\phi_m\rangle = p_m|\phi_m\rangle$, where the eigenvalue $p_m$ is equal to $m\hbar_{\rm eff}$, and the eigenstate $\langle\theta|\phi_m\rangle$ is given by $\langle\theta|\phi_m\rangle = {\rm e}^{{\rm i}m\theta}/\sqrt{2\pi}$, with $m = \ldots,-2,-1,0,1,2,\ldots$. During the time interval from $t = n$ to $t = n+1$, the evolution of the quantum state is govern by $|\psi(t=n+1)\rangle = U|\psi(t=n)\rangle$, with the Floquet operator

$$U = U_{\rm f}U_{\rm K}U_{\rm NL}, \tag{3}$$

where the free evolution operator is defined as

$$U_{\rm f} = \exp\Big(-\frac{\rm i}{\hbar_{\rm eff}}\frac{p^2}{2}\Big), \tag{4}$$

the evolution operator of the kicking term is defined as

$$U_{\rm K} = \exp\Big\{-\frac{\rm i}{\hbar_{\rm eff}}(K+{\rm i}\lambda)[1+\varepsilon\cos(\omega t)]\cos\theta\Big\}, \tag{5}$$

and the nonlinear interaction reads

$$U_{\rm NL} = \exp\Big[-\frac{\rm i}{\hbar_{\rm eff}}g|\psi(p)|^2\Big]. \tag{6}$$

The diffusion behavior of the BEC system in momentum space is characterized by the energy, $\langle p^2\rangle = \frac{1}{\mathcal{N}}{\rm Tr}(\rho p^2)$, where $\mathcal{N} = \sum_m|\psi_m|^2$ is the norm and $\rho = |\psi\rangle\langle\psi|$ is the reduced density matrix of the quantum state. The phase diagram of the diffusion behavior with different values of $\lambda$ and $g$ is shown in Fig. 1. Class I is the DL regime, where $\langle p^2\rangle \propto t^\alpha$ with $\alpha = 0$ under weak nonlinearity ($g < g_{\rm c}$). Class II clarifies the SD regime with $\alpha = 0.4$ for $g > g_{\rm c}$. In this work, we focus on the case of $\lambda > \lambda_{\rm c}$ and find that the diffusion behavior is quantified by a power law

$$\langle p^2\rangle = \beta t^\alpha, \tag{7}$$

where $\beta$ is the diffusion coefficient. Interestingly, the system displays a wide spectrum of energy diffusion from the SBD with $\alpha > 2$, to AD with $1 < \alpha < 2$ and CD with $\alpha = 1$, with the increase of the nonlinearity parameter $g$. Our finding provides new insights into the chaotic dynamics of quantum many-body systems and opens up avenues for further research on the fundamental problems, e.g., quantum thermalization in this field.

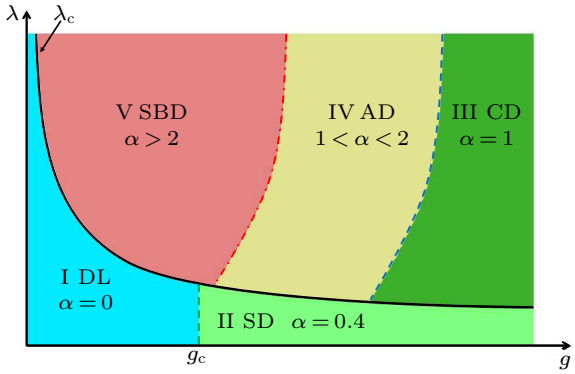



**Fig. 1.** Schematic phase diagram of quantum diffusion ($\langle p^2\rangle \propto t^\alpha$) in the parameter space $(\lambda, g)$. The solid curve of $\lambda_{\rm c}$ denotes the crossover from diffusion phase with interplay between nonlinear interaction and non-Hermitian driving to diffusion phase without interplay. The three dashed lines indicate nonsingular crossover between different diffusion phases with variation of nonlinear interaction. Here $g_{\rm c}$ denotes the threshold of nonlinear interaction strength for the crossover from phase I to phase II. It is slightly dependent on $\lambda$.

## 3. Super-ballistic quantum diffusion induced by nonlinear interaction

### 3.1. Time dependence of mean energy and inverse participation ratio

We numerically investigate the time-dependent mean energy $\langle p^2\rangle$ for various values of $g$, specifically in cases where the non-Hermitian driving potential is sufficiently large. We initialize the system in the ground state, represented as $\psi_0(\theta) = 1/\sqrt{2\pi}$. As depicted in Fig. 2(a), when $g = 0$, the energy diffusion $\langle p^2\rangle$ exhibits DL, which is induced by non-Hermiticity.[45] The corresponding momentum distribution has an exponentially localized shape, $|\psi(p)|^2 \propto {\rm e}^{-|p|/\mu}$ [see Fig. 2(d)], which is a typical characteristic of DL. For weak nonlinearity (e.g., $g = 10^{-3}$), the mean energy follows the DL of $g = 0$ for time smaller than a threshold value $\kappa_{\rm c}$, representing the occurrence of prethermalization. Interestingly, for $t > \kappa_{\rm c}$, quantum diffusion displays the way of SBD, i.e., $\langle p^2\rangle = \beta t^\alpha$ with $\alpha \approx 3.3$.

We observe that the exponent $\alpha$ decreases as $g$ increases, following the relation $\alpha \propto -\ln g$, as illustrated in Fig. 2(c). This relationship suggests a transition in the diffusion from

SBD to AD and then to CD, as demonstrated in Fig. 1. Furthermore, we numerically explore the growth rate $\beta$ across a wide range of $g$ values. Our findings indicate that $\beta$ increases according to a power law with $g$, i.e., $\beta \propto g^{\gamma}$, as shown in Fig. 2(c). This result reveals an enhancement of diffusion due to nonlinear interaction. In this situation, the probability density distribution in momentum space can be expressed as

$$|\psi(p,t)|^2 \propto \begin{cases} \rho(t), & |p| \le p_{\rm c}(t), \\ {\rm e}^{-[|p|-p_{\rm c}(t)]/\sigma}, & |p| > p_{\rm c}(t). \end{cases} \tag{8}$$

This distribution displays a plateau for $|p| < p_{\rm c}$ and exponentially decaying tails for $|p| > p_{\rm c}$ [see Fig. 2(d)]. The width of the plateau, represented by $L(t) = 2p_{\rm c}(t)$, increases with time, signifying the emergence of delocalization.[50,51]

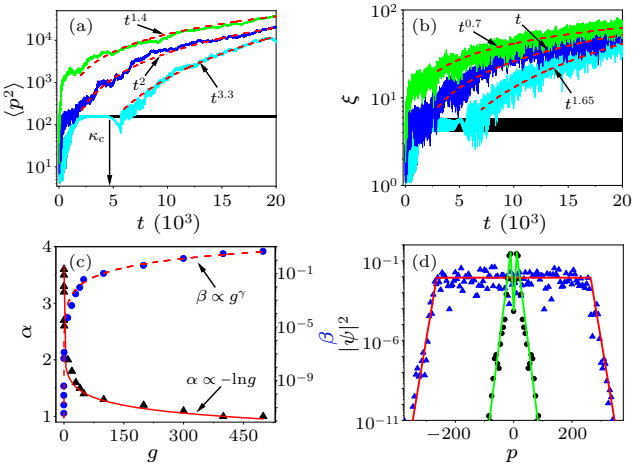



**Fig. 2.** Time evolution of $\langle p^2\rangle$ (a), and $\xi$ (b) with $g = 0$ (black), $10^{-3}$ (cyan), 10 (blue), and 50 (green). Red lines in panels (a) and (b) indicate $\langle p^2\rangle = \beta t^{\alpha}$ and $\xi \propto t^{\alpha/2}$, respectively; $\kappa_{\rm c}$ in panel (a) is the critical time of the pre-thermalization. (c) Dependence of $\alpha$ (triangles) and $\beta$ (circles) on $g$. The red solid (dashed) line indicates the fitting function with the form $\alpha \propto -\ln g$ ($\beta \propto g^{\gamma}$ with $\gamma = 2.3$). (d) Angular momentum distributions $|\psi(p)|^2$ at time $t = 2\times 10^4$ for $g = 0$ (circles) and $g = 10$ (triangles). The green (red) line indicates the fitting function $|\psi(p)|^2 \propto {\rm e}^{-|p|/\mu}$ for $g = 0$ [Eq. (8) for $g = 10$]. Other parameters are $K = 5$, $\hbar_{\rm eff} = 5$, $\varepsilon = 0.1$, and $\lambda = 10^{-2}$.

The inverse participation ratio (IPR) has been widely used to assess the spread of a quantum state and is represented by the equation $\xi = (\sum_m |\psi_m|^2)^2/\sum_m |\psi_m|^4$, with $m = \ldots, -2, -1, 0, 1, 2, \ldots$.[45,52,53] We further investigate the IPR ($\xi$) for various values of $g$. Figure 2(b) shows that the IPR rapidly increases and reaches saturation when $g = 0$. It can be readily deduced that the IPR is proportional to the localization length $\mu$ for an exponentially localized quantum state given by $|\psi(p)|^2 \propto {\rm e}^{-|p|/\mu}$. Notably, the IPR follows a power-law growth with time, i.e., $\xi \propto t^{\alpha/2}$ for nonzero $g$. Here, $\alpha$ represents the exponent of diffusion for the $\langle p^2\rangle$. The relationship between $\xi$ and $\langle p^2\rangle$ can be determined using the probability density distribution provided in Eq. (8). By disregarding the exponentially decaying tails, a rough estimation of $\rho$ corresponding to the plateau of the momentum distribution in Eq. (8) gives $\rho \propto 1/p_{\rm c}$, resulting from normalization. Consequently, we establish the relation $\langle p^2\rangle \sim \xi^2$, which unveils the correlation between the spread of the quantum state and energy diffusion.

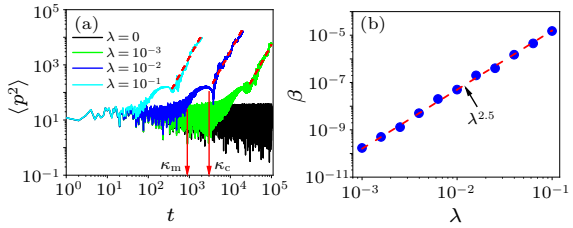



**Fig. 3.** (a) Time evolution of $\langle p^2\rangle$ for different $\lambda$. Red dashed lines indicate the fitting function with the form $\langle p^2\rangle = \beta t^{2.7}$; $\kappa_{\rm m}$ and $\kappa_{\rm c}$ are critical times of pre-thermalization. (b) Dependence of $\beta$ on $\lambda$. The red dashed line indicates the fitting function of the form $\beta \propto \lambda^{\nu}$ with $\nu = 2.5$. Other parameters are $K = 5$, $\hbar_{\rm eff} = 5$, $\varepsilon = 0.1$, and $g = 0.1$.

We further investigate the time evolution of $\langle p^2\rangle$ for various values of the parameter $\lambda$. In the Hermitian case (i.e., when $\lambda = 0$), the energy diffusion exhibits DL, as shown in Fig. 3(a). For a sufficiently strong non-Hermiticity (e.g., $\lambda = 10^{-3}$), the $\langle p^2\rangle$ follows the DL of $\lambda = 0$ for $t < \kappa_{\rm m}$, exhibits a type of prethermalization in the time interval $\kappa_{\rm m} < t < \kappa_{\rm c}$,[54,55] and ultimately increases with an SBD of time $t$, that is, $\langle p^2\rangle = \beta t^{\alpha}$, where the exponent $\alpha$ remains constant as $\lambda$ varies. The diffusive coefficient $\beta$ increases according to a power function, specifically, $\beta \propto \lambda^{\nu}$ with $\nu = 2.5$, as depicted in Fig. 3(b). This demonstrates the enhancement of diffusion by the non-Hermitian driving potential.

### 3.2. Mechanism of super-ballistic diffusion

To reveal the mechanism of super-ballistic diffusion, we examine the norm $\mathcal{N}$ of the quantum state in time evolution for various values of $\lambda$ and $g$. The norm can be used to quantify phase transitions in non-Hermitian systems.[43,56] In the Hermitian system [i.e., $\lambda = 0$ and $g = 0.1$ in Fig. 4(a)], the $\mathcal{N}$ remains at unity throughout the time evolution, demonstrating the conservation of the norm. Correspondingly, the mean energy exhibits DL, as depicted in Fig. 3(a). In the non-Hermitian system without nonlinear interaction [e.g., $\lambda = 10^{-2}$ and $g = 0$ in Fig. 4(a)], the norm decreases slightly for time smaller a threshold value $t_{\rm m}$, beyond which it increases sharply in an exponential function, i.e., $\mathcal{N} \propto {\rm e}^{\eta t}$. We numerically investigate the $t_{\rm m}$ for different $\lambda$. Figure 4(c) demonstrates that $t_{\rm m}$, in perfect consistency with the threshold time $\kappa_{\rm m}$ for the DL of energy diffusion, decays inversely with $\lambda$. This demonstrates that the DL exists prior to the manifestation of non-Hermitian effects.

For nonzero $g$ values (e.g., $g = 0.1$ in Fig. 4(b)), $\mathcal{N}$ follows the behavior of $g = 0$ for times smaller than a threshold value $t_{\rm c}$. Beyond this point, it also increases unboundedly, but at a significantly lower rate compared to the case of $g = 0$. We further investigate the $t_{\rm c}$ for different $g$. Figure 4(d) reveals

that $t_c$ decays logarithmically with $g$, i.e., $t_c \propto -\ln g$, which is in good agreement with the behavior of threshold time $\kappa_c$ for the appearance of the SBD. This demonstrates that the effects of nonlinear interaction becomes predominant for $t > t_c$, leading to the occurrence of the SBD.

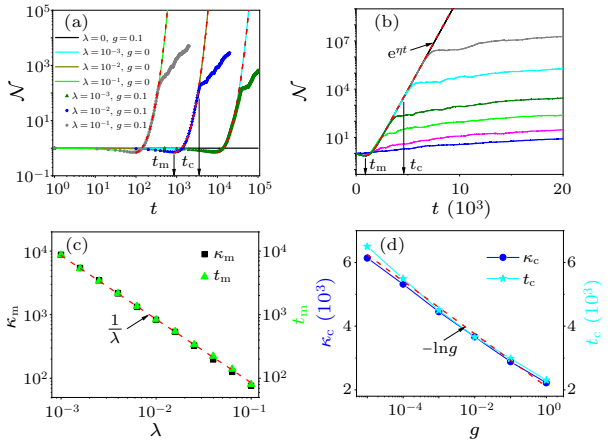



**Fig. 4.** (a) Norm ($\mathcal{N}$) versus time for $g = 0.1$ with different $\lambda$ and $g = 0$ with different $\lambda$. Red dashed lines indicate the fitting function of the form $\mathcal{N} \propto e^{\eta t}$. (b) Norm ($\mathcal{N}$) versus time for $\lambda = 10^{-2}$ with $g = 0$ (black), $10^{-5}$ (gray), $10^{-3}$ (cyan), 0.1 (olive), 1 (green), 10 (magenta), and 50 (blue). Here $t_m$ and $t_c$ in panels (a) and (b) are critical points of $\mathcal{N}$. (c) Dependence of $\kappa_m$ and $t_m$ on $\lambda$ for $g = 0.1$. (d) Dependence of $\kappa_c$ and $t_c$ on $g$ for $\lambda = 10^{-2}$. Red dashed lines in panels (b), (c), and (d) indicate the fitting function of the form $\mathcal{N} \propto e^{\eta t}$ with $\eta = 0.0027$, $t_m(\kappa_m) \propto 1/\lambda$, and $t_c(\kappa_c) \propto -\ln g$, respectively. Other parameters are $K = 5$, $\hbar_{\rm eff} = 5$, and $\varepsilon = 0.1$.

## 4. Summary

We numerically identify several energy diffusion behaviors in the parameter space $(\lambda, g)$ using the QPQKR model for $\lambda > \lambda_c$, specifically, SBD, AD, and CD. The mean energy adheres to a power-law function of time, represented by $\langle p^2 \rangle = \beta t^\alpha$, $\alpha \geq 1$. The diffusion exponent $\alpha$ decreases logarithmically with $g$, while the diffusion coefficient $\beta$ increases with a power law regarding $g$. Interestingly, the system experiences a prethermalization stage before transition to SBD. The time evolution of the norm $\mathcal{N}$ displays two critical times, $t_m$ and $t_c$, which are consistent with the threshold time of $\kappa_m$ of DL and $\kappa_c$ of SBD, respectively. We find that the $t_m$ ($\kappa_m$) decays inversely with $\lambda$, while $t_c$ ($\kappa_c$) decays logarithmically with $g$. Our analysis of $\mathcal{N}$ demonstrates that the interplay between the non-Hermitian driving potential and the nonlinear interaction results in the emergence of SBD.

## Appendix A: Experimental design and non-dimensionalization for the BEC system

The pulsed optical lattice interacting with the BEC of ultra-cold atoms can be represented by $E = 2E_0(t')\cos(k_L X + \pi/2)\cos(w_L t')$. Here, $\omega_L = k_L c = 2\pi c/\lambda_L$ denotes the frequency of the two lasers responsible for forming the light standing wave. The term $E_0(t') = E_0[1 + \varepsilon\cos(\omega_M t')]^{1/2}$, $\omega_M \ll \omega_L$, where $\varepsilon$ and $\omega_M$ represent the quasi-periodic modulation strength and modulation frequency of the laser amplitude $E_0(t')$, respectively. The mean square electric field of the light standing wave, represented by $\overline{E^2}$, is obtained by averaging over a light oscillation period $T_L$. It can be expressed as $\overline{E^2} = (1/T_L)\int_0^{T_L} E^2\,dt' \approx E_0^2[1-\cos(2k_L X)]\cdot[1+\varepsilon\cos(\omega_M t')]$.

Ultra-cold atoms feature two energy levels, $E_1$ and $E_2$, as well as an additional non-interacting energy level $E_i$. A strong decay without radiation occurs from $E_2$ to $E_i$, thereby supplying the non-Hermitian driving potential.[57,58] Simultaneously, the stimulated emission from $E_2$ to $E_1$ with a transition frequency of $\omega_0$ generates the Hermitian driving potential.[48,57,58] As a consequence, the interaction between the optical lattice and the ultra-cold atom can be characterized by the complex potential,[58] denoted as $V_K = p_e^2\overline{E^2}/[\hbar(\Delta + i\gamma/2)]$. Here, $p_e$ represents the electric dipole matrix element for the transition from $E_2$ to $E_1$, the detuning $\Delta(=\omega_L - \omega_0)$ is negative, and $\gamma$ is the loss rate from $E_2$ to $E_i$. By substituting $\overline{E^2}$ into $V_K$, we obtain $V_K = [V_0 + V_X]\cdot[1+\varepsilon\cos(\omega_M t')]$, where $V_0 = -\frac{2p_e^2E_0^2(-2\Delta+i\gamma)}{\hbar(4\Delta^2+\gamma^2)}$ and $V_X = \frac{2p_e^2E_0^2(-2\Delta+i\gamma)}{\hbar(4\Delta^2+\gamma^2)}\cos(2k_L X)$. Offsetting $V_0$ through pumping from both $E_1$ and $E_i$ to $E_2$ yields the relation

$$V_K = \frac{2p_e^2E_0^2(-2\Delta+i\gamma)}{\hbar(4\Delta^2+\gamma^2)}\cdot\cos(2k_L X)\cdot[1+\varepsilon\cos(\omega_M t')]. \tag{A1}$$

We introduce a nonlinear interaction in momentum space, i.e., $V_{NL} = \bar{g}|\psi(P)|^2$.[32] The Hamiltonian of the BEC system considered in this work is given by

$$\mathcal{H} = \frac{P^2}{2M} + V_K\cdot\tau\sum_{n=0}^{\infty}\delta_\tau(t'-nT) + V_{NL}, \tag{A2}$$

where $P = -i\hbar\partial/\partial X$ denotes the momentum of a BEC atom, and the quantum state $|\varphi\rangle$ adheres to a periodic boundary condition in the $X$ space, i.e., $\tilde{\varphi}(X+\lambda_L/2) = \tilde{\varphi}(X)$. In this equation, $T$ represents the pulse period, $\tau(\ll T)$ corresponds to the pulse duration on the atom, and $\delta_\tau(t'-nT) = 1/\tau$ if $|t'-nT| \leq \tau/2$ and 0 otherwise. The momentum $P$ space wave function $\varphi(P)$ and the coordinate $X$ space wave function $\tilde{\varphi}(X)$ are related by the Fourier transformation $\varphi(P) = \int_{-\lambda_L/4}^{\lambda_L/4}\sqrt{2/\lambda_L}e^{-iPX/\hbar}\tilde{\varphi}(X)\,dX$. We define dimensionless variables as $\theta = 2k_L X$, $\hbar_{\rm eff} = 4T\hbar k_L^2/M$, $p = -i\hbar_{\rm eff}\partial/\partial\theta$, $t = t'/T$, $K = -\frac{16p_e^2E_0^2\Delta T k_L^2\tau}{M\hbar(4\Delta^2+\gamma^2)}$, $\lambda = \frac{8p_e^2E_0^2\gamma T k_L^2\tau}{M\hbar(4\Delta^2+\gamma^2)}$, $\omega = \omega_M T$, and $g = \frac{4\bar{g}T^2k_L^2}{M}$.[48] Consequently, the effective Hamiltonian of the QPQKR model can be expressed as

$$H = \frac{p^2}{2} + g|\psi(p)|^2 + V_K(\theta)\sum_n^{\infty}\delta(t-n), \tag{A3}$$

with

$$V_K(\theta) = (K+i\lambda)[1+\varepsilon\cos(\omega t)]\cos\theta. \tag{A4}$$

## Acknowledgments

Jian-Zheng Li is supported by the Science and Technology Research Program of Jiangxi Education Department (Grant No. GJJ190463) and the Doctoral Start-up Fund of Jiangxi University of Science and Technology (Grant No. 205200100067). Wen-Lei Zhao is supported by the National Natural Science Foundation of China (Grant No. 12065009), the Natural Science Foundation of Jiangxi Province (Grant Nos. 20224ACB201006 and 20224BAB201023), and the Science and Technology Planning Project of Ganzhou City (Grant No. 202101095077).

## References

[1] Čadež T, Mondaini R and Sacramento P D 2017 *Phys. Rev. B* **96** 144301
[2] Russomanno A, Fava M and Fazio R 2021 *Phys. Rev. B* **103** 224301
[3] Zhao Q F, Müller C A and Gong J B 2014 *Phys. Rev. E* **90** 022921
[4] Duffy G J, Mellish A S, Challis K J and Wilson A C 2004 *Phys. Rev. A* **70** 041602(R)
[5] Maurya S S, Kannan J B, Patel K, Dutta P, Biswas K, Mangaonkar J, Santhanam M S and Rapol U D 2022 *Phys. Rev. E* **106** 034207
[6] Zhao W L, Gong P K, Wang J Z and Wang Q 2020 *Chin. Phys. B* **29** 120302
[7] An F A, Meier E J and Gadway B 2017 *Nat. Commun.* **8** 325
[8] Kohlert T, Scherg S, Li X, Lüschen H P, Sarma S D, Bloch I and Aidelsburger M 2019 *Phys. Rev. Lett.* **122** 170403
[9] Lucioni E, Deissler B, Tanzi L, Roati G, Zaccanti M, Modugno M, Larcher M, Dalfovo F, Inguscio M and Modugno G 2011 *Phys. Rev. Lett.* **106** 230403
[10] Zhang Z, Tong P, Gong J and Li B 2012 *Phys. Rev. Lett.* **108** 070603
[11] Geraldi A, Laneve A, Bonavena L D, Sansoni L, Ferraz J, Fratalocchi A, Sciarrino F, CuevasÁ and Mataloni P 2019 *Phys. Rev. Lett.* **123** 140501
[12] Sharabi Y, Sheinfux H H, Sagi Y, Eisenstein G and Segev M 2018 *Phys. Rev. Lett.* **121** 233901
[13] Gholami E and Lashkami Z M 2017 *Phys. Rev. E* **95** 022216
[14] Shirley J H 1965 *Phys. Rev.* **138** B979
[15] Bukov M, D'Alessio L and Polkovnikov A 2015 *Adv. Phys.* **64** 139
[16] Santhanam M S, Paul S and Kannan J B 2022 *Phys. Rep.* **956** 1
[17] Lima R and Shepelyansky D 1991 *Phys. Rev. Lett.* **67** 1377
[18] Fishman S, Grempel D R and Prange R E 1982 *Phys. Rev. Lett.* **49** 509
[19] Grempel D R, Prange R E and Fishman S 1984 *Phys. Rev. A* **29** 1639
[20] Casati G, Guarneri I and Shepelyansky D L 1989 *Phys. Rev. Lett.* **62** 345
[21] Lemarié G, Grémaud B and Delande D 2009 *Europhys. Lett.* **87** 37007
[22] Lemarié G, Lignier H, Delande D, Szriftgiser P and Garreau J C 2010 *Phys. Rev. Lett.* **105** 090601
[23] Davis K B, Mewes M O, Andrews M R, Druten N J V, Durfee D S, Kurn D M and Ketterle W 1995 *Phys. Rev. Lett.* **75** 3969
[24] Dalfovo F, Giorgini S, Pitaevskii L P and Stringari S 1999 *Rev. Mod. Phys.* **71** 463
[25] Reitter M, Näger J, Wintersperger K, Sträter C, Bloch I, Eckardt A and Schneider U 2017 *Phys. Rev. Lett.* **119** 200402
[26] Wang L W, Wen K, Liu F D, Li Y D, Wang P J, Huang L H, Chen L C, Han W, Meng Z M and Zhang J 2022 *Chin. Phys. B* **31** 103401
[27] Chabé J, Lemarié G, Grémaud B, Delande D, Szriftgiser P and Garreau J C 2008 *Phys. Rev. Lett.* **101** 255702
[28] White D H, Haase T A, Brown D J, Hoogerland M D, Najafabadi M S, Helm J L, Gies C, Schumayer D and Hutchinson D A W 2020 *Nat. Commun.* **11** 4942
[29] Cherroret N, Vermersch B, Garreau J C and Delande D 2014 *Phys. Rev. Lett.* **112** 170603
[30] Lellouch S, Rançon A, Bièvre S D, Delande D and Garreau J C 2020 *Phys. Rev. A* **101** 043624
[31] Vermersch B, Delande D and Garreau J C 2020 *Phys. Rev. A* **101** 053625
[32] Ermann L and Shepelyansky D L 2014 *J. Phys. A: Math. Theor.* **47** 335101
[33] Zhang C W, Liu J, Raizen M G and Niu Q 2004 *Phys. Rev. Lett.* **92** 054101
[34] Toh J H S, McCormick K C, Tang X X, Su Y, Luo X W, Zhang C W and Gupta S 2022 *Nat. Phys.* **18** 1297
[35] Cao A, Sajjad R, Mas H, Simmons E Q, Tanlimco J L, Martinez E N, Shimasaki T, Kondakci H E, Galitski V and Weld D M 2022 *Nat. Phys.* **18** 1302
[36] Ashida Y, Gong Z P and Ueda M 2020 *Adv. Phys.* **69** 249
[37] Moiseyev N 2011 *Non-Hermitian Quantum Mechanics* (Cambridge: Cambridge University Press) p. 1
[38] Li Y, Peng Y G, Han L, Miri M A, Li W, Xiao M, Zhu X F, Zhao J L, Alú A, Fan S and Qiu C W 2019 *Science* **364** 6436
[39] Ganainy R E, Makris K G, Khajavikhan M, Musslimani Z H, Rotter S and Christodoulides D N 2018 *Nat. Phys.* **14** 11
[40] Gao T, Estrecho E, Bliokh K Y, Liew T C H, Fraser M D, Brodbeck S, Kamp M, Schneider C, Höfling S, Yamamoto Y, Nori F, Kivshar Y. S, Truscott A. G, Dall R G and Ostrovskaya E A 2015 *Nature* **526** 554
[41] Keller C, Oberthaler M K, Abfalterer R, Bernet S, Schmiedmayer J and Zeilinger A 1997 *Phys. Rev. Lett.* **79** 3327
[42] Li J M , Harter A K, Liu J, Melo L D, Joglekar Y N and Luo L 2019 *Nat. Commun.* **10** 855
[43] Longhi S 2017 *Phys. Rev. A* **95** 012125
[44] Huang K Q, Wang J Z, Zhao W L and Liu J 2021 *J. Phys.: Condens. Matter* **33** 055402
[45] Huang K Q, Zhao W L and Li Z 2021 *Phys. Rev. A* **104** 052405
[46] Zhao W L, Zhou L W, Liu J, Tong P Q and Huang K Q 2020 *Phys. Rev. A* **102** 062213
[47] Gadway B, Reeves J, Krinner L and Schneble D 2013 *Phys. Rev. Lett.* **110** 190401
[48] Lemarié G, Chabé J, Szriftgiser P, Garreau J C, Grémaud B and Delande D 2009 *Phys. Rev. A* **80** 043626
[49] See appendix for the experimental realization of the quasi-periodic kicked rotor model with ultral-cold atoms.
[50] Shepelyansky D L 1993 *Phys. Rev. Lett.* **70** 1787
[51] Pikovsky A S and Shepelyansky D L 2008 *Phys. Rev. Lett.* **100** 094101
[52] Wegner F 1980 *Z. Phys. B* **36** 209
[53] Liu T, Cheng S J, Zhang R, Ruan R R and Jiang H X 2022 *Chin. Phys. B* **31** 027101
[54] Rajak A, Dana I and Torre E G D 2019 *Phys. Rev. B* **100** 100302(R)
[55] Kundu A, Rajak A and Nag T 2021 *Phys. Rev. B* **104** 075161
[56] Zhao W L , Wang J Z, Wang X H and Tong P Q 2019 *Phys. Rev. E* **99** 042201
[57] Li J Z, Zhao W L and Liu J 2023 *Phys. Rev. A* **107** 032208
[58] Oberthaler M K, Abfalterer R, Bernet S, Schmiedmayer J and Zeilinger A 1996 *Phys. Rev. Lett.* **77** 4980